Environmental Science and Pollution Research (2020) 27:44306–44313
https://doi.org/10.1007/s11356-020-10364-4

RESEARCH ARTICLE

Effective biosorption of uranium from aqueous solution by cyanobacterium *Anabaena flos-aquae*

Yijun Yuan[1] · Nana Liu[1] · Ying Dai[1] · Binliang Wang[2] · Yunzhi Liu[1] · Chuanhong Chen[1] · Dejuan Huang[1]

Received: 12 June 2020 / Accepted: 3 August 2020 / Published online: 6 August 2020

Abstract

Anabaena flos-aquae, a typical species of cyanobacterial bloom, was employed as a useful biosorbent for uranium removal. Batch experiments were conducted to examine the effects of different parameters on the uranium uptake amount of *Anabaena flos-aquae*. The maximum adsorption capacity of 196.4 mg/g was obtained under the optimized experimental conditions. The calculations of kinetic and thermodynamic results proved the adsorption process was endothermic, chemisorption, and spontaneous. The adsorption of uranium onto *Anabaena flos-aquae* was better defined by the Langmuir model, which indicated the process was a monolayer sorption. In addition, the characterization of the biosorbent before and after uranium sorption implied that the dominant functional groups participated in the uranium adsorption process were hydroxyl, amino, and carboxyl. In conclusion, the environmentally friendly and biocompatible characteristics of *Anabaena flos-aquae* suggest that it can be a promising biosorbent for uranium removal.

Keywords *Anabaena flos-aquae* · Uranium · Biosorption · Thermodynamic · Isotherm

Introduction

Due to the excessive amounts of heavy metal produced by anthropogenic activities discharged into the environment, the pollution of heavy metals has aroused wide concern. Among the major categories of heavy metals, radionuclides, known for its chemical toxicity and radiotoxicity, has gained wide public attention. Uranium, as the important source materials of nuclear energy, can be easily detected in the environment due to effluents from the smelting of uranium ore and normal discharge of radioactive waste from nuclear power plants (Ogar et al. 2014; Gudkov et al. 2016).Unfortunately, uranium is inhaled and ingested by human beings eventually through the food chain. Once consuming more than tolerated levels of uranium, it can lead to an increase risk of lots of diseases and physical deformities (ATSDR 2013; Soltani et al. 2019). Meanwhile, the non-renewable characteristics of uranium may prevent the sustainable utilize of nuclear energy (Li et al. 2016). Therefore, it is crucial to remove and recover of uranium from polluted water efficiently.

Traditional methods of uranium removal and recovery include solvent extraction (Cheira 2020; Mathuthu et al. 2019), chemical precipitation (Djedidi et al. 2009), reverse osmosis (Abdel-Khalek et al. 2011; Schulte-Herbrueggen et al. 2016), micellar ultrafiltration (Cojocaru et al. 2009), and adsorption. These methods mentioned above have been demonstrated effective in the field of uranium-contaminated wastewater treated. However, limitations of these methods, such as high energy consumption, secondary pollution, and incomplete removal, are unfavorable to the widespread popularization and promotion of these methods. Among these methods, adsorption gains an advantage over other methods owing to its high efficiency and environmentally friendly.

Biosorption is an adsorption process that utilizes biological materials as adsorbents (Ghasemi et al. 2011). Over the past decades, biosorption has attracted great attentions owe to its unparalleled advantage, such as simplicity, repeatability, eco-friendly, and so on (Yi et al. 2016). In recent years, many

Yijun Yuan and Nana Liu contributed equally to this work.

Yijun Yuan and Nana Liu should be considered co-first authors.

Responsible Editor: Tito Roberto Cadaval Jr

✉ Yijun Yuan
yuanyijun@ecut.edu.cn

[1] State Key Laboratory of Nuclear Resources and Environment, East China University of Technology, Nanchang 330013, China

[2] School of Life Science, Shaoxing University, Huancheng West Road 508, Shaoxing 312000, China

biosorbents are being widely used in uranium wastewater treatment, for instance, *Citrus limon* peels (Šabanović et al. 2019), *Saccharomyces cerevisiae* (Zheng et al. 2018), and *Lemna* sp. (Vieira et al. 2019). Among the biosorbents mentioned above, microalgae possess incomparable technical advantages. Firstly, the cultivation of algae is relatively simple (Hu et al. 2011). Secondly, it is easier be harvested because of widely distributed, locally abundant, and much larger size than bacteria (Yu et al. 2014). Finally, and most importantly, it has been confirmed that microalgae have a strong affinity for metals. The functional groups on the cell wall such as carboxyl and amino are important sites for the microorganism to bind metals (Vilar et al. 2008; He and Chen 2014). Recently, freshwater or marine algae, such as *Spirulina platensis* (Mohammed 2019), *Gracilaria corticata* (Dabbagh et al. 2018), *Cystoseira* sp. (Cem et al. 2017), *Cladophora hutchinsiae* (Bagda et al. 2017), and brown algae (Moghaddam et al. 2013), attracted a great deal of attention for uranium removal. However, according to our literature survey, rarely investigation on the biosorption of uranium by *Anabaena flos-aquae* has been reported.

Anabaena flos-aquae, a species of filamentous cyanobacteria, is known for its nitrogen-fixing abilities and is one of cyanobacterial species that produce toxins. If it could be harvested and played a vital role in the uranium-containing wastewater treatment, then we can realize a "win-win situation." The influences of various experimental parameters on the biosorption of uranium were investigated. The characterization of raw and U-loaded *Anabaena flos-aquae* was performed by Fourier transform infrared spectroscopy (FTIR), scanning electron microscopy (SEM), and energy dispersive X-ray fluorescence spectrometry (EDS).

Materials and methods

Preparation of biosorbent

Anabaena flos-aquae strain was obtained from the Freshwater Algae Culture Collection at the Institute of Hydrobiology, Chinese Academy of Sciences. The cells of *Anabaena flos-aquae* were cultivated in BG-11 medium in a fermenter until the end of the exponential growth phase. The biomass was then harvested by centrifugation and washed twice with distilled water. Afterwards, the precipitate was freeze-dried, passed through a 100-size mesh, and finally preserved in desiccator for following experimental use.

Batch experiments

All adsorption experiments were duplicated at least to make reliable and repeatable results. The experiments were performed by setting the reaction mixture of *Anabaena flos-aquae* (10 mg) and 30 mL uranium solution of certain concentration into a conical flask, so as to characterize specific sorption parameters: initial pH, contact time, initial uranium concentration, and environmental temperature. The initial pH (2–8) was adjusted with trace amount of NaOH and HNO_3. The effects of different gradient of *Anabaena flos-aquae* dose (10, 20, 30, 40, 50, 60, 80, 100 mg) on uranium biosorption were studied. Then, the mixture was rotated at 120 rpm in a rotary shaker. The uranium concentration in the supernatant was determined at 650 nm with UV-Vis spectrophotometer after centrifugation. The removal efficiency (R) and sorption amount (Q) of uranium were calculated by Eq. (1) and Eq. (2).

$$R(\%) = \frac{C_0 - C_e}{C_0} \times 100\% \quad (1)$$

$$Q = \frac{(C_0 - C_e) \times V,}{m} \quad (2)$$

where C_0 and C_e are the initial uranium concentration and equilibrium uranium concentration (mg/L), respectively; V is the volume of the solution (L); and m is the mass of the absorbent (g).

Characterization

The surface morphology of *Anabaena flos-aquae* was examined by SEM (GeminiSEM 300) coupled with EDS (operating conditions: probe current 45 nA, accelerating voltage 20 kV and counting time 60 s). The samples were gold-coated before observation to enhance the electrical conductivity. Functional groups on the surface of *Anabaena flos-aquae* were observed using FTIR (Bruker Vector 22). To perform FTIR analysis, sample disks were prepared by mixing 0.15 g potassium bromide (KBr) with 0.005 g dry *Anabaena flos-aquae* and pressed into tablet form. Then, the spectra were recorded over the 400–4000 cm^{-1} region with a resolution of 0.2 cm.

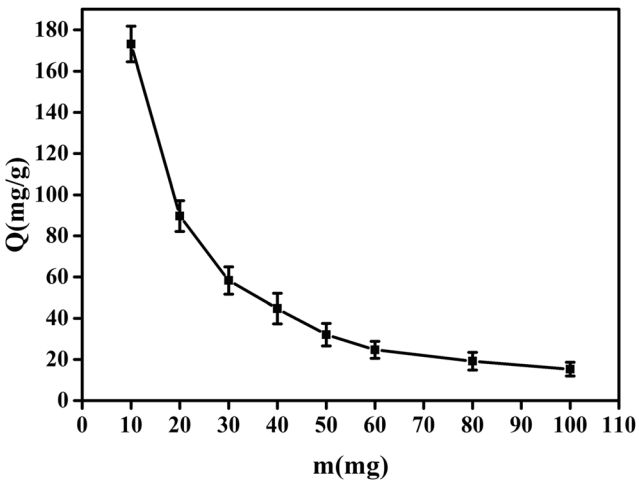

Fig. 1 The effect of sorbent dose on the uranium adsorption by *Anabaena flos-aquae* (C_0 = 70 mg/L, t = 1 h, V = 30 mL, T = 298.2 K, pH = 5.0)

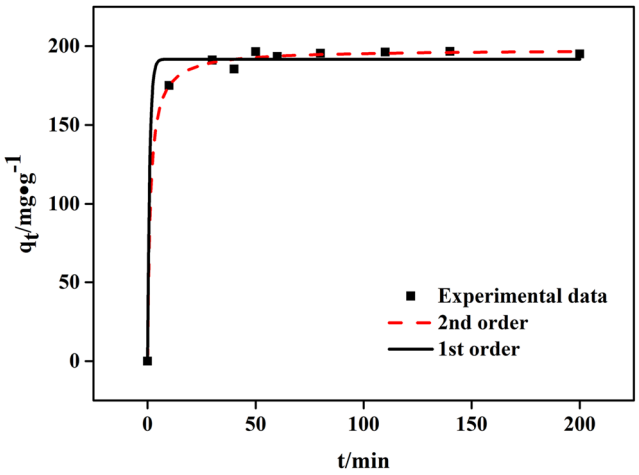

Fig. 2 Kinetics of uranium adsorption onto *Anabaena flos-aquae* (C_0 = 70 mg/L, m = 10 mg, V = 30 mL, T = 298.2 K, pH = 5.0)

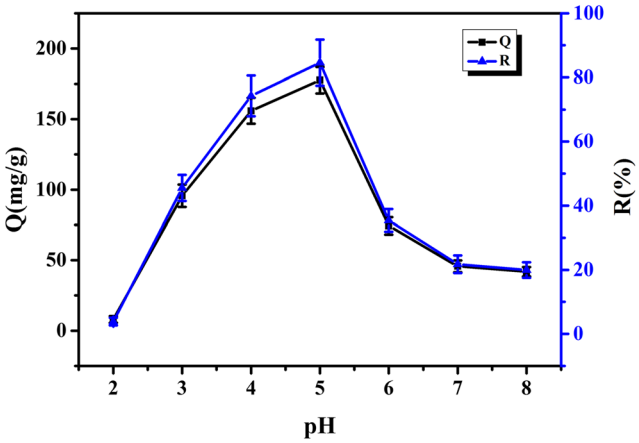

Fig. 3 The effect of pH on the uranium adsorption by *Anabaena flos-aquae* (C_0 = 70 mg/L, m = 10 mg, V = 30 mL, T = 298.2 K, t = 60 min)

Results and discussion

Effect of biomass dose

As presented in Fig. 1, the adsorption capacity decreased with the increase of biomass dose. The maximum biosorption capacity was 173.06 mg/g with 10 mg biomass dose. Similar results have been reported regarding the effect of biomass dose on biosorption capacity (Li et al. 2016). The negative relationship between biosorption capacity and biomass dose may result from the aggregate effect of sorbents (Deng et al. 2011). A "screening effect" that increased electrostatic interactions between cells, limited availability of binding sites, and reduced mixing generated by the higher sorbent dose results in a lower uranium sorption per unit of sorbent. In conclusion, 10 mg of *Anabaena flos-aquae* is appropriate for the following uranium biosorption experiments.

Kinetic studies

The influence of contact time on uranium biosorption was investigated. As shown in Fig. 2, the adsorption capacity increased sharply during the first 20 min and then reached equilibrium of maximum uranium sorption amount 196.4 mg/g at 50 min. Therefore, the reaction time of 1 h was employed in the following experiments.

The pseudo-first-order model and the pseudo-second-order model were employed to describe the adsorption kinetic characteristic. The two models can be expressed by the following Eq. (3) and Eq. (4).

$$\text{Pseudo-first-order}: q_t = q_e\,(1-\exp(-k_1 t)) \tag{3}$$

$$\text{Pseudo-second-order}: q_t = \frac{t}{\left(1/k_2 q_e^2\right) + (t/q_e)} \tag{4}$$

where q_e is the uranium uptake amount at equilibrium, and q_t refers to the uranium adsorption capacity at any time "t"; k_1 and k_2 refer to the rate constant of the pseudo-first-order and pseudo-second-order sorption, respectively. The parameters obtained by the two models are presented in Table 1.

Table 1 shows the correlation coefficient (R^2) of the pseudo-second-order model is higher than the value of the pseudo-first-order model. Meanwhile, the calculated q_e value of pseudo-second-order model (197.71 mg/g) was approximate to the value measured by the experiment ($Q_{e,\exp}$ = 196.4 mg/g). It indicated that the adsorption process is more favor of the pseudo-second-order model, which implying that adsorption process could be chemisorption (Idris et al. 2013; Humelnicu et al. 2011).

Table 1 The parameters of two models for uranium adsorption onto *Anabaena flos-aquae*

Pseudo-first-order	
q_e (mg/g)	191.63
k_1 (min^{-1})	1
R^2	0.989
Pseudo-second-order	
q_e (mg/g)	197.71
$k_2 \times 10^3$ (min^{-1})	5.97
R^2	0.998

Table 2 Adsorption isotherm parameters calculated with Langmuir and Freundlich models

Adsorbents	Langmuir			Freundlich		
	K_L (L/mg)	q_m (mg/g)	R^2	K_F	n_F	R^2
Anabaena flos-aquae	0.12	190.1	0.992	49.58	3.3	0.882

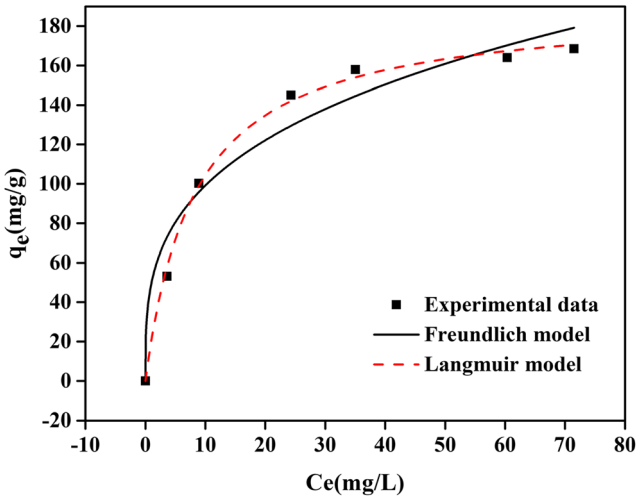

Fig. 4 Isotherm models of uranium biosorption by *Anabaena flos-aquae*. The solid lines are Freundlich model simulation, and the dashed lines are Langmuir model simulation

Effect of pH

pH was demonstrated one of the most important parameters influencing the metal adsorption (Ghorbani et al. 2008; Gok and Aytas 2009). The uranium removal efficiency (R) and uranium sorption amount (Q) increased dramatically with an increasing pH from 2 to 5 as can been seen in Fig. 3. The removal efficiency of uranium at pH 2 was nearly 3.8%, and corresponding uranium sorption amount was 8.06 mg/g. When pH ascent from 2 to 5, the maximum uranium removal efficiency (R) of 84.6% and uranium sorption amount of 177.6 mg/g were observed at pH 5. The increasing positivity of the adsorbents, the electrostatic repulsion between positively charged uranyl cations, and high concentrations of H^+ in the reaction mixture result in the low adsorption capacity at lower pH (Ai et al. 2013; Cao et al. 2013). With increasing pH, an increase of negative charges owes to the deprotonated on the *Anabaena flos-aquae*, finally enhanced the biosorption of positively charge uranium on the cell surface of *Anabaena flos-aquae*. However, when the pH was above 5, the biosorption of uranium decreased gradually. The decline of the uranium sorption efficiency may result from the formation of precipitate ($4UO_3{\cdot}9H_2O$) when the pH is higher than 5 (Ghorbani et al. 2008; Khani 2011). Therefore, the optimum pH (pH = 5) for subsequent uranium adsorption on *Anabaena flos-aquae* experiments was selected.

Table 3 Thermodynamic data of uranium adsorption onto *Anabaena flos-aquae*

ΔH (kJ/mol)	ΔS (J/(K mol))	ΔG (kJ/mol)		
		288.2 K	298.2 K	308.2 K
21.83	100.18	− 28.85	− 29.85	− 30.85

Adsorption isotherm

To illuminate the mechanism of the adsorption process, the Langmuir and Freundlich model analyses were conducted. Langmuir isotherm is commonly applied to describe monolayer adsorption (Foo and Hameed 2010; Ding et al. 2014). In contrast, the Freundlich model assumes multilayer sorption on the heterogeneous surface (Foo and Hameed 2010; Xiong et al. 2013). The two models can be expressed by Eq. (5) and Eq. (6).

$$\text{Langmuir}: q_e = \frac{q_m k_L C_e}{1 + k_L C_e} \tag{5}$$

$$\text{Freundlich}: q_e = k_F C_e^{1/n_F} \tag{6}$$

where C_e refers to the equilibrium concentration (mg/L) and q_e refers to the equilibrium adsorption capacity(mg/g), q_m is the maximum adsorption capacity(mg/g), and K_L is the constant related to the energy of adsorption; K_F and n_F denote the Freundlich constant and Freundlich exponent, respectively.

The value of q_e increased firstly and then reached equilibrium state later with the concentration increased, which revealed that the initial concentration provides a driving force

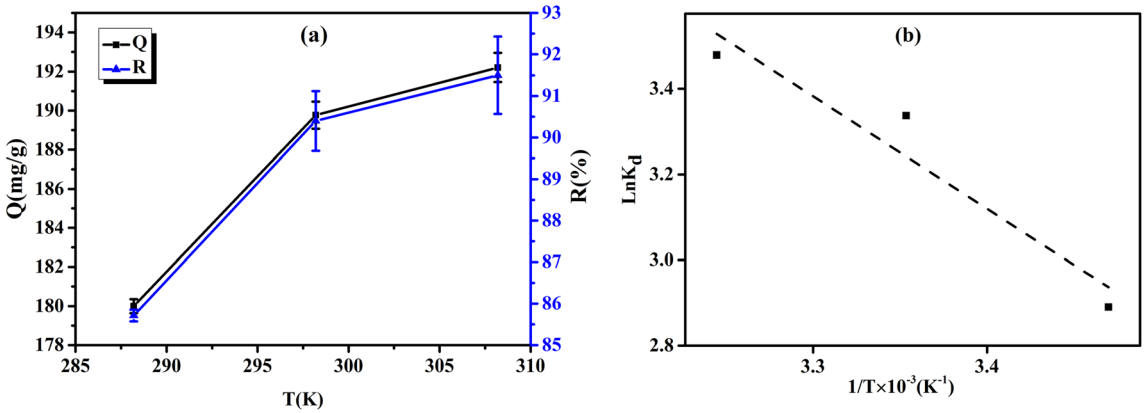

Fig. 5 The effect of temperature on the uranium adsorption by *Anabaena flos-aquae* (**a**) and plot of lnK_d against 1/T (**b**)

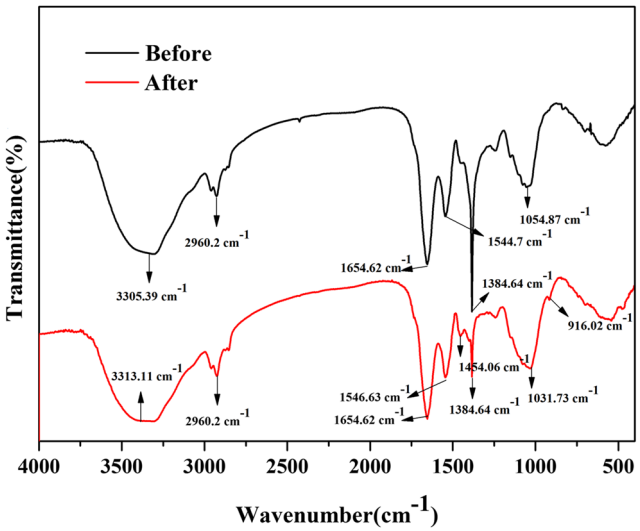

Fig. 6 The FTIR spectra of *Anabaena flos-aquae* before and after uranium adsorption

for uranium adsorbed onto *Anabaena flos-aquae* (Han et al. 2018; Gok and Aytas 2009). The parameters presented in Table 2 were calculated from the linear curves presented in Fig. 4. The higher R^2 value of the Langmuir isotherm model and the sorption capacity calculated from the Langmuir model ($q_m = 190.1$ mg/g) which was the approach to the value measured by the experiment (168.5 mg/g) both indicate that the biosorption of uranium onto *Anabaena flos-aquae* can be well described by the Langmuir model. Based on the isotherm analysis, it was confirmed that the uranium adsorption process onto *Anabaena flos-aquae* was likely monolayer coverage.

Notably, the biosorption capacity of adsorbents was always evaluated by the value of the maximum adsorption capacity (q_m). For example, the q_m for *Dictyopteris polypodioides* was 62.5 mg/g (Bampaiti et al. 2016), 113.5 mg/g for *Saccharomyces cerevisiae* (Faghihian and Peyvandi 2012), 152 mg/g for *Cladophora hutchinsiae* (Bagda et al. 2017), and 97.15 mg/g for *Chlorella vulgaris* (Amini et al. 2012).

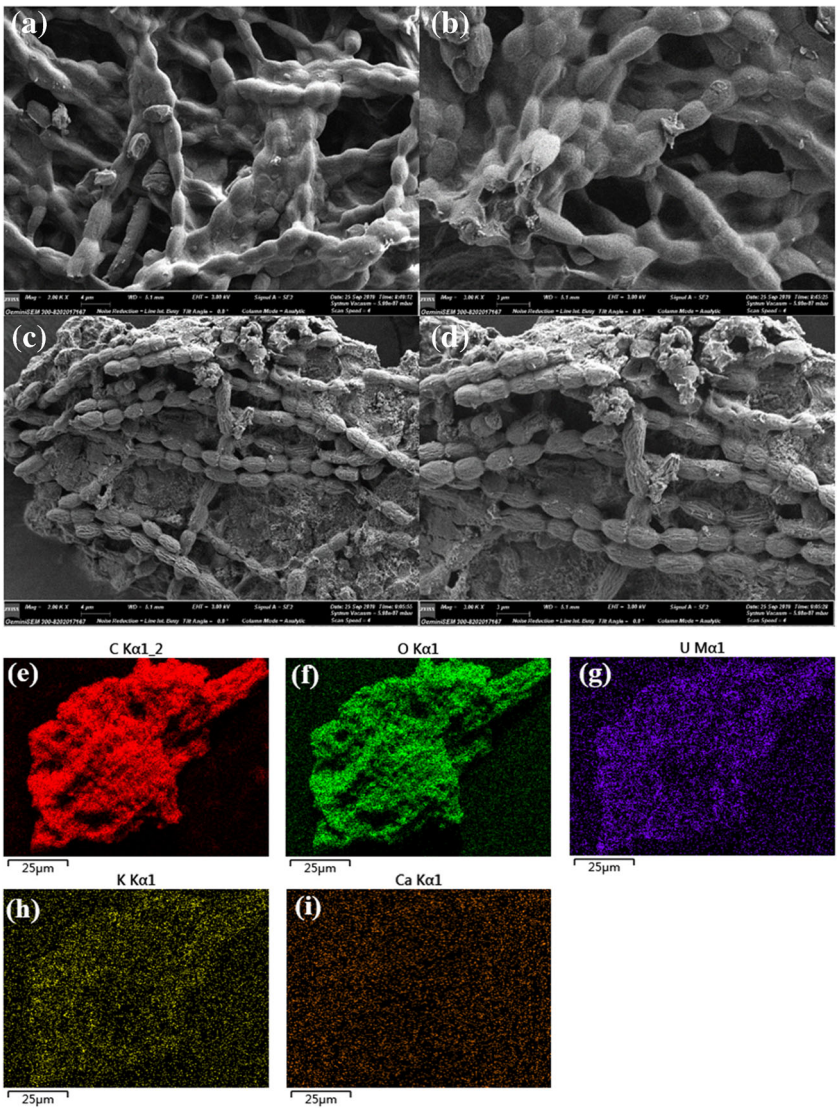

Fig. 7 SEM images of *Anabaena flos-aquae* before (**a** magnification of × 2000, **b** magnification of × 3000) and after adsorption(**c** magnification of × 2000, **d** magnification of × 3000); mapping of *Anabaena flos-aquae* after adsorption (**e** carbon, **f** oxygen, **g** uranium, **h** potassium, **i** calcium)

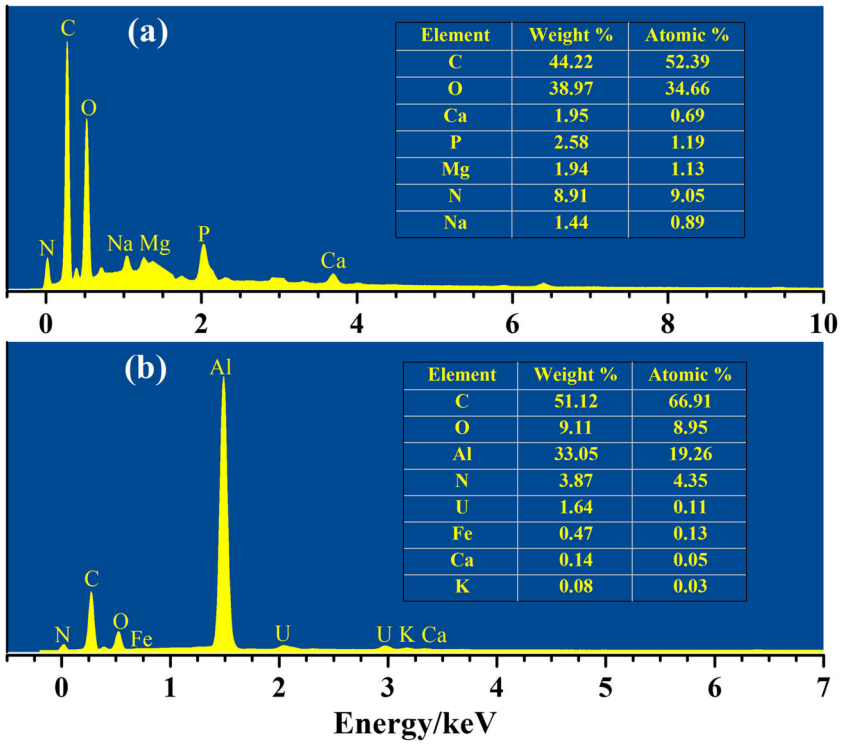

Fig. 8 EDS analysis of *Anabaena flos-aquae* before (**a**) and after (**b**) uranium adsorption

Evidently, a comparison of the maximum capacities among these adsorbents proved the *Anabaena flos-aquae* has a considerable high biosorption capacity for uranium. Besides, the low operational cost and maximization of benefits give the *Anabaena flos-aquae* more advantages over lots of adsorbents.

Adsorption thermodynamics

In order to figure out the influence of temperature on the adsorption reaction, the adsorption experiments at different temperatures (288.2 K, 298.2 K, and 308.2 K) were conducted. As presented in Fig. 5a, the amount of uranium adsorbed onto *Anabaena flos-aquae* increased gradually with the increase of temperature, which demonstrating the adsorption process may be endothermic. Thermodynamic parameters were calculated using the equations given below and listed in Table 3.

$$\mathrm{Ln}K_d = \frac{\Delta S}{R} - \frac{\Delta H}{\mathrm{RT}} \tag{7}$$

$$\Delta G = \Delta \mathrm{H} - T\Delta S \tag{8}$$

$$K_d = q_e / C_e \tag{9}$$

where K_d refers to the equilibrium constant and R represents gas constant (8.314 J mol^{-1} K^{-1}); T refers to the absolute temperature in Kelvin (K). The enthalpy and entropy were calculated from the plot of $\ln K_d$ against 1/T in Fig. 5b. The positive values of ΔH and ΔS proved the adsorption process was endothermic and the increased randomness at the solid-solution interface (Bozkurt et al. 2011; Saleem and Bhatti 2011; Donat 2009). Meanwhile, the negative value of ΔG suggests the adsorption process was spontaneous. In conclusion, the thermodynamic study revealed that the biosorption of uranium onto *Anabaena flos-aquae* was endothermic and spontaneous.

Characterization of *Anabaena flos-aquae*

FTIR spectra of *Anabaena flos-aquae*

To characterize specific functional groups involved in biosorption, the FTIR patterns of *Anabaena flos-aquae* were recorded before and after sorption of uranium. For the *Anabaena flos-aquae*, the bands at approximately 3305.39 cm^{-1} corresponded to the O-H and N-H stretching vibrations. The peaks at 1654.62 cm^{-1} and 1544.7 cm^{-1} were ascribed to the N-H stretching of amino groups. The band at 1054.87 cm^{-1} were assigned to the C-OH stretching (Yi et al. 2016).

For the U-loaded *Anabaena flos-aquae*, the peaks at 1054.87, 1544.7, and 3305.39 cm^{-1} correspond to -COOH, -NH_2, and -OH shifted to 1031.73, 1546.63, and 3313.11 cm^{-1}, respectively (Fig. 6). It implied that the -COOH, -NH_2, and -OH performed an important role in uranium biosorption. Furthermore, two new peaks at 1454.06 cm^{-1} and 916.02 cm^{-1} were observed. The two peaks represented the stretching frequency of the structure that formed by U

atoms combined with oxygen-containing functional groups (Xie and Gao 2007; Zhang et al. 2014; Zhao et al. 2019).

SEM-EDS of *Anabaena flos-aquae*

The SEM images of *Anabaena flos-aquae* before and after uranium loaded were shown in Fig. 7. As can be seen from the micrographs of raw *Anabaena flos-aquae* with magnification of × 2000 and × 3000 in Fig. 7a, b, the morphology of pure *Anabaena flos-aquae* is smooth and flat. As presented in Fig. 7c, d, the surface became rough because of the formation of many deep grooves after exposure to uranium. These grooves may give the *Anabaena flos-aquae* more chance to accommodate considerable uranyl ions.

The element content of the sample before and after uranium sorption was analyzed by EDS. According to EDS analysis in Fig. 8a, b, the algae was mainly consisted of carbon (49%), oxygen (36%), and nitrogen (11%) as well as small quantities of sodium, magnesium, phosphorus, and calcium. After exposure to uranium, the uranium peak was detected (1.64%). Besides, the atomic percentage of nitrogen (3.87%) and oxygen (9.11%) decreased. The combination of SEM-EDS and FTIR data indicates that uranium has been successfully adsorbed by *Anabaena flos-aquae*.

Conclusion

As a common species of cyanobacteria bloom, *Anabaena flos-aquae* was utilized for the biosorption of uranium in this study. The maximum uranium sorption amount was found to reach the value of 196.4 mg/g. The biosorption of uranium onto *Anabaena flos-aquae* was well fitted to the Langmuir isotherm model and pseudo-second-order model, which proved the adsorption process was monolayer sorption and chemisorption. The results of thermodynamic analysis indicated that uranium uptake was endothermic and spontaneous. The FTIR results demonstrated that the -OH, -NH_2, and -COOH performed an important role in uranium biosorption. In conclusion, the effective biosorption of uranium from aqueous solution by cyanobacterium *Anabaena flos-aquae* makes it a promising, environmentally friendly, and biocompatible biosorbent for the treatment of uranium contaminants.

Funding information This work is financially supported by Natural Science Foundation of Jiangxi Province (No. 20192BAB214005; No. 20181BAB214005) and National Natural Science Foundation of China (Grant No. 41867063).

References

Abdel-Khalek AA, Ali MM, Ashour RM, Abdel-Magied AF (2011) Chemical studies on uranium extraction from concentrated phosphoric acid by using PC88A and DBBP mixture. J Radioanal Nucl Chem 290:353–359

Ai L, Luo X, Lin X, Zhang S (2013) Biosorption behaviors of uranium (VI) from aqueous solution by sunflower straw and insights of binding mechanism. J Radioanal Nucl Chem 298:1823–1834

Amini M, Younesi H, Bahramifar N (2012) Biosorption of U (VI) from aqueous solution by *Chlorella vulgaris*: equilibrium, kinetic, and thermodynamic studies. J Environ Eng 139:410–421

ATSDR (Agency for Toxic Substances and Disease Registry) (2013) Toxicological profile for Uranium. **Available online at**: http://www.atsdr.cdc.gov/ToxProfiles/tp150.pdf

Bagda E, Tuzen M, Sari A (2017) Equilibrium, thermodynamic and kinetic investigations for biosorption of uranium with green algae (*Cladophora hutchinsiae*). J Environ Radioact 175:7–14

Bampaiti A, Yusan S, Aytas S, Pavlidou E, Noli F (2016) Investigation of uranium biosorption from aqueous solutions by *Dictyopteris polypodioides* brown algae. J Radioanal Nucl Chem 307:1335–1343

Bozkurt SS, Molu ZB, Cavas L, Merdivan M (2011) Biosorption of uranium (VI) and thorium (IV) onto Ulva gigantea (Kützing) bliding: discussion of adsorption isotherms, kinetics and thermodynamic. J Radioanal Nucl Chem 288:867–874

Cao Q, Liu Y, Wang C, Cheng J (2013) Phosphorus-modified poly (styrene-codivinylbenzene)-PAMAM chelating resin for the adsorption of uranium (VI) in aqueous. J Hazard Mater 263:311–321

Cem G, Aytas S, Sezer H (2017) Modeling uranium biosorption by *Cystoseira* sp. and application studies. Sep Sci Technol 52:792–803

Cheira F (2020) Solvent extraction of uranium and vanadium from carbonate leach solutions of ferruginous siltstone using cetylpyridinium carbonate in kerosene. Chem Pap 74:2247–2266. https://doi.org/10.1007/s11696-020-01073-w

Cojocaru C, Zakrzewska-Trznadel G, Miskiewicz A (2009) Removal of cobalt ions from aqueous solutions by polymer assisted ultrafiltration using experimental design approach part 2: optimization of hydrodynamic conditions for a crossflow ultrafiltration module with rotating part. J. Hazard.Mater 169:610–620

Dabbagh R, Rojaee A, Heshmatipour Z (2018) Thermodynamics, kinetics and equilibrium studies of uranium sorption by *Gracilaria corticata* red alga. Environ Eng Manag J 17:1199–1208

Deng H, Lu J, Li G, Zhang G, Wang X (2011) Adsorption of methylene blue on adsorbent materials produced from cotton stalk. Chem Eng J 172:326–334

Ding C, Cheng W, Sun Y, Wang X (2014) Determination of chemical affinity of graphene oxide nanosheets with radionuclides investigated by macroscopic, spectroscopic and modeling techniques. Dalton Trans 43:3888–3896

Djedidi Z, Bouda M, Souissi MA, Cheikh RB, Mercier G, Tyagi RD, Blais JF (2009) Metals removal from soil, fly ash and sewage sludge leachates by precipitation and dewatering properties of the generated sludge. J HazardMater 172:1372–1382

Donat R (2009) The removal of uranium (VI) from aqueous solutions onto natural sepiolite. J Chem Thermodyn 41:829–835

Faghihian H, Peyvandi S (2012) Adsorption isotherm for uranyl biosorption by Saccharomyces cerevisiae biomass. J Radioanal Nucl Chem 293:463–468

Foo KY, Hameed BH (2010) Insights into the modeling of adsorption isotherm systems. Chem Eng J 156:2–10

Ghasemi M, Keshtkar AR, Dabbagh R, Safdari SJ (2011) Biosorption of uranium (VI) from aqueous solutions by Ca-pretreated Cystoseira indica alga: break through curves studies and modeling. J Hazard Mater 189:141–149

Ghorbani F, Younesi H, Ghasempouri SM, Zinatizadeh AA, Amini M, Daneshi A (2008) Application of response surface methodology for optimization of cadmium biosorption in an aqueous solution by Saccharomyces cerevisiae. Chem Eng J 145:267–275

Gok C, Aytas S (2009) Biosorption of uranium (VI) from aqueous solution using calcium alginate beads. J Hazard Mater 168:369–375

Gudkov SV, Chernikov AV, Bruskov VI (2016) Chemical and radiological toxicity of uranium compounds. Russ. J. General Chem 86: 1531–1538

Han B, Zhang E, Cheng G, Zhang L, Wang D, Wang X (2018) Hydrothermal carbon superstructures enriched with carboxyl groups for highly efficient uranium removal. Chem Eng J 338:734–744

He J, Chen J (2014) A comprehensive review on biosorption of heavy metals by algal biomass: materials, performances, chemistry, and modeling simulation tools. Bioresour Technol 160:67–78

Hu H, Li X, Yu Y, Wu Y, Sagehashi M, Sakoda A (2011) Domestic wastewater reclamation coupled with biofuel/biomass production based on microalgae: a novel wastewater treatment process in the future. J Water Environ Technol 9:199–207

Humelnicu D, Dinu MV, Drăgan ES (2011) Adsorption characteristics of UO_2^{2+} and Th^{4+} ions from simulated radioactive solutions onto chitosan/clinoptilolite sorbents. J Hazard Mater 185:447–455

Idris S.A., Alotaibi K.M., Peshkur T.A., Anderson P., Morris M., Gibson L.T (2013) Adsorption kinetic study: effect of adsorbent pore size distribution on the rate of Cr (VI) uptake. Micropor Mesopor Mater 165:99–105

Khani MH (2011) Statistical analysis and isotherm study of uranium biosorption by *Padina* sp. algae biomass. Environ. Sci. Pollut. Res 18:790–799

Li F, Li D, Li X, Liao J, Li S, Yang J, Yang Y, Tang J, Liu N (2016) Microorganism-derived carbon microspheres for uranium removal from aqueous solution. Chem Eng J 284:630–639

Mathuthu M, Mokhine ND, Stassen E (2019) Organic solvent extraction of uranium from alkaline nuclear waste. J Radioanal Nucl Chem 319:687–693

Moghaddam MR, Fatemi S, Keshtkar A (2013) Adsorption of lead (Pb^{2+}) and uranium (UO_2^{2+}) cations by brown algae: experimental and thermodynamic modeling. Chem Eng J 231:294–303

Mohammed AAER (2019) Potentiality of quercetin-sodium hydroxide modified Spirulina platensis in uranium biosorption from waste effluent. Int J Environ Stud 77:1–13

Ogar A, Grandin A, Sjoberg V, Turnau K, Karlsson S (2014) Stabilization of uranium (VI) at low pH by fungal metabolites: applications in environmental biotechnology. APCBEE Procedia 10: 142–148

Šabanović E, Muhić-Šarac T, Nuhanović M, Memić M (2019) Biosorption of uranium (VI) from aqueous solution by Citrus limon peels: kinetics, equlibrium and batch studies. J Radioanal Nucl Chem 319:425–435

Saleem N, Bhatti HN (2011) Adsorptive removal and recovery of U(VI) by citrus waste biomass. BioResources 6:2522–2538

Schulte-Herbrueggen HMA, Semiao AJC, Chaurand P, Graham MC (2016) Effect of pH and pressure on uranium removal from drinking water using nf/ro membranes. Environ Sci Technol 50:5817–5824

Soltani M, Zarei MH, Salimi A, Pourahmad J (2019) Mitochondrial protective and antioxidant agents protect toxicity induced by depleted uranium in isolated human lymphocytes. J Environ Radioact 203: 112–116

Vieira LC, de Araujo LG, de Padua Ferreira RV, da Silva EA, Canevesi RLS, Marumo JT (2019) Uranium biosorption by *Lemna* sp. and *Pistia stratiotes*. J Environ Radioact 203:179–186

Vilar VJP, Botelho CMS, Boaventura RAR (2008) Lead and copper biosorption by marine red algae Gelidium and algal composite material in a CSTR ("Carberry" type). Chem Eng J 138:249–257

Xie X, Gao L (2007) Characterization of a manganese dioxide/carbon nanotube composite fabricated using an in situ coating method. Carbon 45:2365–2373

Xiong Y, Xu J, Shan W, Lou Z, Fang D, Zang S, Han G (2013) A new approach for rhenium (VII) recovery by using modified brown algae *Laminaria japonica* adsorbent. Bioresour Technol 127:464–472

Yi Z, Yao J, Chen H, Wang F, Yuan Z, Liu X (2016) Uranium biosorption from aqueous solution onto *Eichhornia crassipes*. J Environ Radioact 154:43–51

Yu J, Zhao W, Yang G, Zeng S (2014) Research on biological materials with uranium biosorption by microalgae: a review. Appl Mech Mater 508:290–296

Zhang S, Shu X, Zhou Y, Huang L, Hua D (2014) Highly efficient removal of uranium (VI) from aqueous solutions using poly (acrylic acid)-functionalized microspheres. Chem Eng J 253:55–62

Zhao C, Liu J, Deng Y, Tian Y, Sun Q (2019) Uranium (VI) adsorption from aqueous solutions by microorganism-graphene oxide composites via an immobilization approach. J Clean Prod 236:117624

Zheng X, Shen Y, Wang X, Wang T (2018) Effect of pH on uranium (VI) biosorption and biomineralization by Saccharomyces cerevisiae. Chemosphere 203:109–116